Electronic transitions in bulk $Al_{0.3}Ga_{0.7}As$ under hydrostatic pressure

W. Patrick Roach,* Meera Chandrasekhar, and H. R. Chandrasekhar
Department of Physics and Astronomy, University of Missouri, Columbia, Missouri 65211

F. A. Chambers
Amoco Technology Corporation, P.O. Box 400, Naperville, Illinois 60566
(Received 15 April 1991)

We present a study of the radiative transitions in $Al_{0.3}Ga_{0.7}As$ under hydrostatic pressure in the range 0–70 kbar using photoluminescence at 15 to 125 K. A new trapping center is reported. The center forms an efficient carrier trap, and produces a pressure-induced hysteresis in the intensity of the radiative transitions. A generic large-lattice-relaxation model with an unusually large emission barrier is proposed to understand the strong hysteresis. We postulate that the center is higher than the X conduction band at ambient pressures, and present arguments to show that it is indeed a different center, not caused by either the DX or the shallow-donor centers. We have also obtained pressure coefficients of several direct and indirect transitions. The activation energies of various radiative transitions and an understanding of the scattering processes at chosen pressures is obtained from the temperature dependence of the luminescence intensities.

I. INTRODUCTION

$Al_xGa_{1-x}As$ has been one of the best studied III-V ternary alloys owing to its technological value and the many interesting phenomena it exhibits. These alloys have properties that make them attractive for the fabrication of heterojunction devices such as lasers, light emitting diodes, and high mobility transistors. One of the important limiting factors in the III-V semiconductors is the presence of deep donor levels. A deep level that has been the focus of several theoretical and experimental investigations[1,2] since its identification[3] in 1977 is the DX center.

One of the fundamental properties of interest is the behavior of deep levels as the band structure is changed with alloying. The binding energies of the levels change dramatically[4] as the alloy changes from a direct to an indirect-band-gap semiconductor around $x=0.38$. In this paper we investigate the shallow and deep levels in $Al_xGa_{1-x}As$ as the band structure is changed from direct to indirect by the application of hydrostatic pressure. Hydrostatic pressure is a fundamental thermodynamic tool that has been used to alter band gaps and the associated impurity levels in a continuously tunable fashion. In $Al_xGa_{1-x}As$, the band ordering changes from Γ–L–X to X–L–Γ as a function of either composition or pressure. A pressure study allows the investigation of the band and impurity related levels as the conduction-band ordering is changed in a *single sample,* where the number of impurities, defects, etc. remains unchanged. This is in contrast to the large number of samples required for an equally detailed investigation where composition is the parameter that is changed. The use of a single sample is vital where the intensity of the radiative transitions has to be monitored as the band structure is changed.

In the present work a study of the intensity of radiative transitions has led to the uncovering of another type of trapping center. The center becomes active at 50 kbar, and quenches all radiative transitions. Upon increasing the pressure to 70 kbar and then reducing it, the radiative intensity does *not* recover until low pressures are reached. The center is found to have a very deep emission barrier, much deeper than DX, and does not empty even at 300 K. We will present arguments to show that this trapping state is not due to the known DX and shallow-donor (SD) centers, dislocations, or level crossings.

Pressure coefficients of the various electronic transitions are obtained, and several indirect deep transitions are identified using laser power density and temperature-dependent studies. Activation energies of various levels at several pressures in the direct and indirect regimes are obtained. A comparison is made between the photoluminescence (PL) intensities of the indirect transitions in the bulk sample and the indirect but staggered transitions in a quantum well, in order to estimate the efficiency with which electrons transfer across the heterointerface.

The paper is organized as follows. Section II presents experimental details. Section III A discusses pressure coefficients of electronic transitions. Section III B discusses the trapping center. Section III C compares the PL efficiency in bulk and quantum-well samples. Section III D presents results on the temperature studies and the activation energies obtained. Section IV is a conclusion.

II. EXPERIMENTAL DETAILS

Photoluminescence from unintentionally doped bulk $Al_{0.3}Ga_{0.7}As$ (10^{15} Si/cm^3) is studied in a pressure range of 0 to 70 kbar and a temperature range of 15 to 125 K. The $Al_{0.3}Ga_{0.7}As$ layer was 2.5-μm thick, grown on a 0.5-μm GaAs buffer layer by molecular-beam epitaxy on

a GaAs substrate. PL was excited by the 5145- and 4880-Å lines of an Ar^+ laser. Laser powers of 0.014 to 15 mW were incident on a spot 30 to 50 μm in diameter. A 0.85-m double grating monochromator with a cooled GaAs photomultiplier tube and photon counting electronics was used to spectrally analyze the emitted radiation. Measurements under hydrostatic pressure were performed in a Merrill-Bassett-type diamond anvil cell with argon as the pressure transmitting medium. A He refrigerator was used to cool the cell. Ruby flourescence was used as the *in situ* manometer. Further details are published elsewhere.[5]

III. RESULTS AND DISCUSSION

Bulk $Al_{0.3}Ga_{0.7}As$ is a direct gap semiconductor at atmospheric pressure, and becomes indirect at ~ 14 kbar where the Γ and X conduction bands (CB's) cross (Sec. III A). A typical PL spectrum at 15 K, using the 5145-Å laser line, is shown in Fig. 1 (inset). At 1 bar, the dominant structure is due to the neutral donor bound exciton

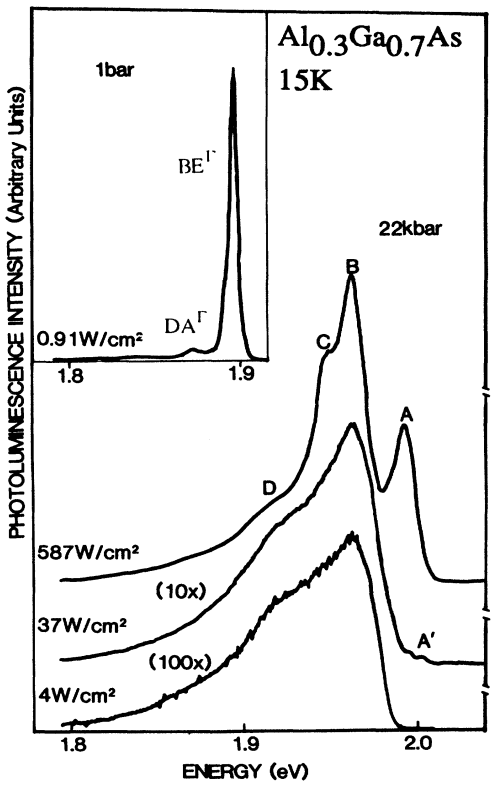

FIG. 1. PL spectra at 1 bar (inset) and 22 kbar at 15 K, excited using the 5145-Å laser line. The Γ bound exciton and DA^{Γ} recombination are observed in the direct regime at 1 bar. These transitions give way to features associated with the indirect CB's at higher pressures. In the region where the X CB is dominant, 22 kbar, the spectra consist of the X donor bound exciton, BE^X (peak A), and DA^X recombination (peaks B, C, and D) at high excitation intensities. At lower intensities, the free exciton FE^X (peak A') is observed. The power densities were calculated assuming a spot 50 μm in diameter.

(BE^{Γ}). The linewidth of BE^{Γ} was 1.6 meV at 15 K and the PL signal was intense (1.6×10^5 counts/s when excited with 15 μW of 5145-Å radiation). Weaker peaks due to a donor-acceptor recombination (DA^{Γ}) from the hydrogenlike shallow donor to an acceptor 22 meV above the VB are also observed at lower energies. These transitions are similar to the DA recombination seen by Dingle.[6] The binding energy of the acceptor suggests[7] that it is C_{As}. The activation energy of the DA^{Γ} peaks obtained from an analysis of PL intensity as a function of temperature (Sec. III D) confirms an activation energy of 21 ± 5 meV.

At pressures above the Γ-X crossover the PL spectra change radically. Levels associated with the indirect X CB appear. These peaks are considerably weaker in intensity, and exhibit a strong dependence on excitation intensity. Spectra at 22 kbar for a few sample laser powers are shown in Fig. 1. At the highest laser powers employed, the spectrum at 15 K shows a bound exciton (BE^X) labeled A and deeper localized levels labeled B, C, and D.

In an attempt to identify these peaks, we study the spectra as a function of incident laser power density. At a low power density, 4.0 W cm^{-2} in Fig. 1, two broad peaks B and D are observed. As the laser power is increased to 37 W cm^{-2}, the intensity of peak B grows relative to that of D, and two weaker peaks A and A' appear at higher energies. At the highest laser power densities, peak A grows rapidly, masking A', while peak D's intensity relative to B declines. A shoulder, peak C, is also seen on the lower-energy side of B. From their peak energy positions, pressure, and temperature behavior, A' is identified as the free exciton (FE^X) and A the neutral donor bound exciton (BE^X) associated with the X CB minimum. Peaks B and D are DA^X recombination peaks that arise from donor levels.

In Fig. 2 the intensities of all peaks are shown as a function of exciting laser intensity at 22 kbar. The linear sections of the curves in the low power density region are fit to the expression $I=\sigma^m$, where I is the PL intensity in counts per second and σ is the incident power density calculated for a 50-μm-diameter spot in units of W cm^{-2}. The laser power was measured at the sample position, and corrected for the reflection losses at the air-diamond and diamond-argon interfaces. The highest power density of 746 W cm^{-2} corresponds to 15 mW of laser power on the sample. From fits to the linear region, we obtain $m=0.64$ for peaks B and C, $m=0.37$ for peak D, and $m=3$ for peak A. The uncertainty in m is about 20%.

From the values of m obtained, it is evident that B and C increase in intensity at the same rate while D grows more slowly. From Fig. 2, it is also clear that D saturates at lower powers than B. The different m values and earlier saturation suggest that peaks B and D arise from two different donor levels, and that D is not a phonon replica of B. This identification is confirmed by the activation energies: the scattering processes to the CB are the same for C and B, but not for D. B and C probably terminate on the same acceptor level C_{As}. The saturation of peak D at low laser powers suggests that D is due to an impurity or defect level with relatively few available states. There-

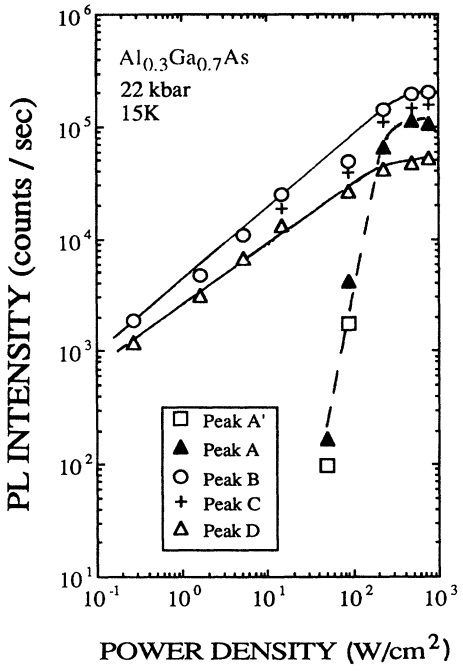

FIG. 2. Intensities of peaks A', A, B, C, and D as a function of exciting intensity at 15 K and 22 kbar. Note that the bound exciton (A) is observed only above a power density of 37 W/cm^2, corresponding to a laser power of 0.7 mW, and that the saturation for D begins at lower powers than that for B and C.

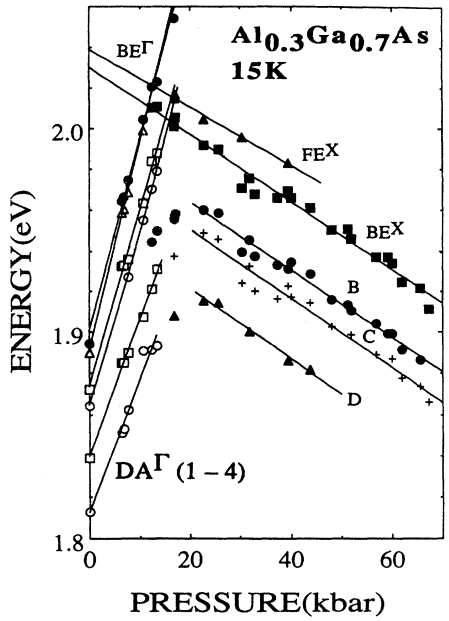

FIG 3. Energies of the peaks in the PL spectra of $Al_{0.3}Ga_{0.7}As$ at 15 K as a function of pressure from 0 to 70 kbar. Note the appearance of transitions from deep donor levels beyond 9 kbar, which show a bowing in the region of the Γ-X crossover.

fore, it saturates at low laser powers, after which recombination from B and C is seen.

Peak C is distinct when the signal-to-noise ratio of the spectrum is good, at the higher laser powers. It tracks peak B in intensity, temperature, and pressure. We therefore assign peak C as a phonon replica. Its energy separation of 10 meV below B indicates that it is assisted by the TA($X \rightarrow K$) phonon.

When B and C are sufficiently populated, the higher energy levels A and A' are seen. At still higher powers A (BE^X) increases rapidly with a large exponent m and becomes the dominant peak, dwarfing A' (FE^X). The laser power, then, provides a sensitive tool for selectively enhancing the various peaks. Conversely, the recombination efficiency can be gauged from the shape of the spectra, along with the PL intensity itself. This feature will be used in a later discussion in Sec. III B.

A. Energies of radiative transitions under pressure

The peak energies of the transitions observed at 15 K are displayed as a function of pressure in Fig. 3. In the pressure range of ~0 to 9 kbar levels tied principally to the Γ CB are observed. The pressure coefficients are listed in Table I. The pressure coefficients of BE$^\Gamma$ obtained are in good agreement with previous works.[8–10] We believe that the previous value of 9.9±0.1 meV/kbar is a more accurate value because of the better statistics in that set of data, as well as more even sampling over the ~14-kbar pressure range over which the BE$^\Gamma$ peak is observed. The $DA^\Gamma(3)$ and $DA^\Gamma(4)$ peaks are weak shoulders whose energies cannot be determined with accuracy. They are, however, shown in Fig. 3 to indicate the pressure at which they disappear and give way to the indirect peaks.

In the intermediate pressure range of ~9 to 20 kbar, where L-X mixing occurs, one sees the evolution of the deep levels B, C, and D, as well as the levels tied to the X CB minimum FE^X (A') and BE^X (A) above 13 kbar. The highest-energy peak FE^X crosses BE$^\Gamma$ at 12.5 kbar. Assuming FE^X is 30 meV below the X CB and BE$^\Gamma$ is 10 meV below the Γ CB, the Γ-X *band* crossing occurs at 14 kbar. While BE^X and FE^X shift linearly in energy with pressure through the entire pressure range, the DA^X levels exhibit a bowing in the vicinity of the crossover due to L-X mixing.

The pressure coefficients obtained are listed in Table I, fit to linear functions for all peaks. We found that fits to a second-order function gave virtually the same residual sum of squares as the first-order fits for all observed levels. For example, for the BE^X (peak A), the residual sum of squares for both fits was exactly the same, 3.4×10^{-4}. The first-order fit is listed in Table I. The second-order fit gave $E(0)=2.0294\pm0.0022$ eV, $\alpha=-1.62\pm0.28$ meV/kbar, and $\beta=-4.5\times10^{-7}\pm3.5\times10^{-6}$ meV/kbar^2. We therefore used the criterion that the lowest-order fit

TABLE I. Pressure coefficients of the peaks in $Al_{0.3}Ga_{0.7}As$, fit to $E(P)=E(0)+\alpha P$.

Transition	$E(0)$ (eV)	α (meV/kbar)	Pressure range (kbar)
BE^{Γ}	1.9001±0.0033	9.47±0.32	0-18
$DA^{\Gamma}(1)$	1.8731±0.0025	8.76±0.27	0-15
$DA^{\Gamma}(2)$	1.8637±0.0015	8.56±0.15	0-15
$DA^{\Gamma}(3)$	1.8398±0.0018	6.64±0.19	0-15
$DA^{\Gamma}(4)$	1.8125±0.0045	6.43±0.50	0-15
FE^{X}	2.0388±0.0025	−1.43±0.09	15-40
BE^{X}	2.0300±0.0022	−1.65±0.05	15-70
DA (B)		−1.65±0.06	20-70
DA (C)		−1.68±0.08	20-70
DA (D)		−1.72±0.12	20-50
	Previous works (nominally $x=0.3$)		
BE^{Γ}	1.872±0.002	9.9±0.1	0-20, 8 K[a]
BE^{X}	2.013±0.003	−0.93±0.09	15-42, 8 K[a]
Band gap (Γ)		10.8±0.1	0-10, 300 K[b]

[a]References 8 and 9.
[b]Reference 10.

was adequate unless the residual sum of squares decreased for a higher-order fit. In the case of $Al_xGa_{1-x}As$, linear fits gave the lowest residual sum of squares. This is not necessarily true of other materials, particularly for direct transitions observable over large pressure ranges.[11]

It is evident from the bowing of B, C, and D between 9 and 20 kbar (Fig. 2) that the levels are resonant above the Γ CB at ambient pressures. However, the data we have in the region of the bowing did not allow us to quantitatively define a second- or higher-order term and accurately establish the energies of the levels at 1 bar. Therefore only linear pressure coefficients in the pressure range of $20<P<70$ kbar are obtained, and $E(0)$ is not quoted for these levels in Table I. It is important to realize that though the α's of the deeper levels are close to those of BE^X, their energies are considerably lower. Similar line shapes are seen in quantum wells, with similar laser power dependence.[12] Remembering that BE^X is not observed until higher laser powers are used, it is vital to properly identify the levels from their shapes, particularly when staggered transitions are used to calculate the VB offset in quantum wells.

We note that the energy of level D at crossover (14 kbar) is about 120 meV below the band crossing, after accounting for the 22-meV downshift in the transition energy since it terminates on an acceptor rather than on the VB. This is consistent with the binding energy of the DX^0 center, calculated to be ~150 meV following the prescription of Ref. 1. Apart from the coincidence in the depths below the CB, there exists no clear evidence to link D to the DX center.

B. A deep center in $Al_{0.3}Ga_{0.7}As$

While the energies of the X associated levels follow a predictable pattern, their PL intensities show rather unusual behavior. Levels B, C, and D have a high and steady intensity up to about 45 kbar. At ~50 kbar, the PL intensity from these levels abruptly drops, and decreases by two orders of magnitude around 70 kbar. Upon reducing the pressure from 70 kbar (downstroke), a surprising result is observed. The PL intensities of the levels tried to the X CB *do not recover* following the same path along which they decreased. In fact, recovery of PL intensity does not occur until very low pressures are achieved (~10 kbar).

A localized center in bulk $Al_{0.3}Ga_{0.7}As$, observed for the first time to the best of our knowledge, is believed to cause this phenomenon. In this section we will present evidence to show that a simple model of a trapping center can explain this pressure-induced hysteresis, and furthermore, that this center is not any of the known centers such as the normal DX or SD centers, but a different type of center.

Substitutional group-IV and -VI dopants in $Al_xGa_{1-x}As$ give rise to two types of electronic states. One is a shallow hydrogenic level and the other is a more localized level, the DX center, believed to arise from lattice distortion near the donor. The relative stability of these states depends on alloy composition.[1] At $x<0.22$ the localized state is a resonance above the Γ CB. At higher Al compositions, the DX center becomes a bound state and more stable than the shallow-donor level. The application of hydrostatic pressure has an effect similar to increasing Al composition. The Γ CB moves up in energy, making the DX a stable state[13–16] at finite pressures for $x<0.22$. In GaAs this shallow-deep transition occurs at 24 kbar.

The center we observe in this work is qualitatively reminiscent of some of the properties of the DX center. The center is resonant above the conduction band, in this case above the X CB minimum, at pressures below 40 kbar. In contrast, the DX is resonant above the Γ CB. At higher

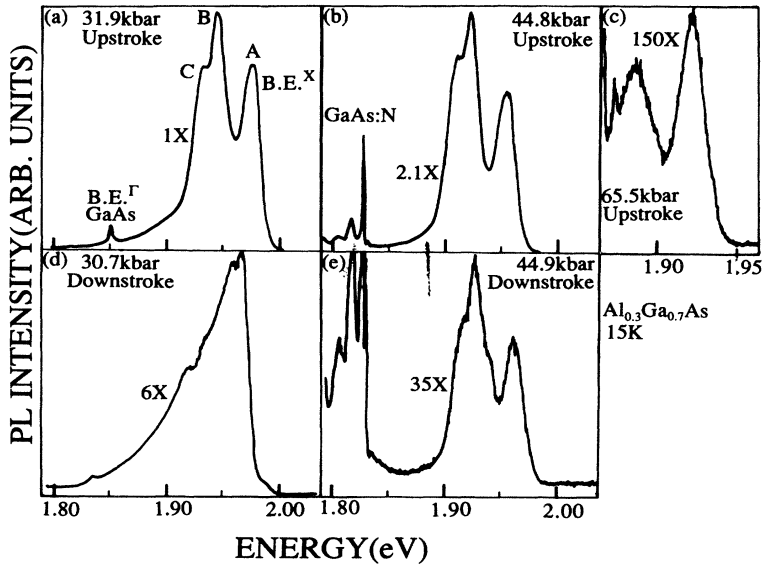

FIG 4. PL spectra in the indirect regime showing the hysteresis in the intensity. In panels (a) and (b) (upstroke) the PL intensity remains relatively constant. Beyond ~50 kbar it drops sharply. At 65 kbar, panel (c), it has decreased by about two orders of magnitude. Upon decreasing the pressure (downstroke) the PL intensity does not recover, as seen in panels (d) and (e), which show spectra at almost the same pressure as (a) and (b), respectively. Note the presence of the transitions due to GaAs:N in the substrate: they are dwarfed by $Al_xGa_{1-x}As$ at 44 kbar in the upstroke, panel (b), while the reverse is true in the downstroke, panel (e). The intensities of GaAs:N serve as an internal calibrant, and show that the loss of intensity is not due to misalignment of the sample. Recovery of intensity ultimately takes place at very low pressures, < 10 kbar.

pressures the center becomes stable and captures all electrons that are photoexcited into the X CB, causing a sharp drop in the PL intensity. When pressure is reduced, to PL intensity does not recover despite thermal cycling to room temperature. This indicates a trapping center with an unusually deep emission barrier, much deeper than that of the DX center.

The decline in PL intensity and the hysteresis observed upon pressure cycling have been repeatedly seen in both a bulk $Al_{0.3}Ga_{0.7}As$ and in a $GaAs/Al_{0.3}Ga_{0.7}As$ MQW sample.[17] A typical spectrum observed in the bulk $Al_{0.3}Ga_{0.7}As$ sample beyond the Γ-X crossover, for increasing pressure (upstroke) is shown in Fig. 4(a) at 32 kbar. The high-energy peak A is the exciton bound to the X CB, BE^X, while the broad peaks B, C, and D are DA^X recombinations described in Sec. III A. Figures 4(a) and 4(b) show that these peaks are quite intense up to ~45 kbar. At ~65 kbar the PL intensity has declined by two orders of magnitude. Note that the intensities in Figs. 4(b)–4(e) are normalized to that of Fig. 4(a).

The unusual hysteresis in the intensity occurs when the pressure is reduced (downstroke). An example is shown in Figs. 4(d) and 4(e), where the spectra are contrasted to those at almost the same pressures as in Figs. 4(a) and 4(b) (upstroke). Pressurizing the sample to 70 kbar and then decreasing the pressure has reduced the observed PL intensity by a factor of 17 at 44 kbar [compare Figs. 4(b) and 4(e)]. The peak energy positions and the spectral line shapes remain the same in the upstroke and downstroke spectra at 44 kbar. At 31 kbar the intensity ratio has improved to a factor of 6 [Figs. 4(a) and 4(d)], however, the line shape has changed drastically.

A plot of PL intensity versus pressure is seen in Fig. 5. The sharp decline in the intensity indicates that another level has crossed the BE^X and DA levels so that recombination occurs via a nonradiative process. As the pressure is reduced, recovery of the PL intensity finally occurs below 10 kbar where BE^Γ dominates the spectrum.

Several plausible causes were explored to explain the decline in PL intensity and the pressure-induced hysteresis effect. A decrease in PL intensity due to a level crossing is a common feature. It was used in GaAs, for example, to establish the Γ-X crossover pressure.[18,19] When the Γ and X bands cross, electrons scatter preferentially to the X CB, the Γ-VB recombination decreases by several orders of magnitude. The same process is observed when the Γ and X CB's cross in $Al_{0.3}Ga_{0.7}As$ as shown in the low-pressure region Fig. 5.

Another example is the crossing of the deep levels of substitutional nitrogen in GaAs with the X CB near 70 kbar.[20] When the nitrogen levels become resonant with the X CB their intensity drops. As in the case of BE^Γ, the GaAs:N transitions reappear upon decreasing the pressure with the same intensity and at the same pressure as in the upstoke. We see these transitions from the GaAs substrate layer [Figs. 4(b) and 4(c)]. The decline and recovery of the GaAs:N PL intensity is shown in Fig. 6, and is markedly different from the hysteresis observed in $Al_xGs_{1-x}As$. Therefore, the hysteresis in the PL intensi-

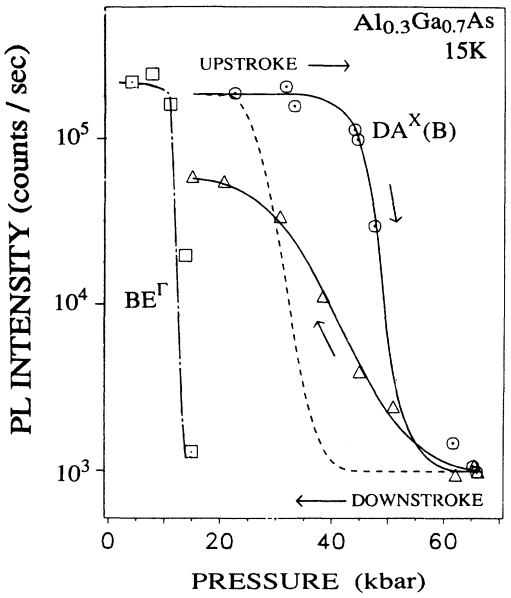

FIG. 5. PL intensities as a function of pressure from 0 to 70 kbar showing the hysteresis effect from 20 to 70 kbar for upstroke and downstroke. BE^{Γ} spectra were excited with 0.91 W/cm^2 while spectra in the indirect regime were excited with 587 W/cm^2. The circles represent the upstroke data, and the triangles the downstroke for the main peak (B) in the indirect regime. The solid lines through the data points are the fits discussed in the text. The dashed line is the recovery curve expected if the pressure were changed at 15 K (see text). In the low-pressure region (10 to 20 kbar), the drop in intensity of BE^{Γ} (squares) is due to the crossing of the Γ and X CB's. The line through the squares is a fit to a function similar to Eq. (1), but with the parameters appropriate to the Γ-X crossing

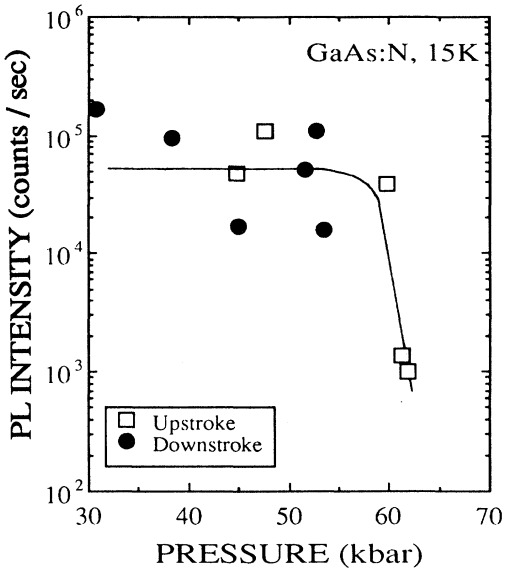

FIG. 6. The PL intensity of the main peak of the GaAs:N transitions. Note that the intensity drops at 62 kbar in the upstroke, but has recovered to its original value at 55 kbar in the downstroke, with no indication of a hysteresis. The scatter in the data is mainly because the PL intensity was optimized for the $Al_xGa_{1-x}As$ rather than for the GaAs peaks in each pressure run.

ty rules out a simple level crossing.

The GaAs:N levels from the substrate seen at 44 kbar, Figs. 4(b) and 4(e), provide an internal calibration of the $Al_{0.3}Ga_{0.7}As$ intensities. The $Al_{0.3}Ga_{0.7}As$ levels overshadow them in the upstroke regime [Fig. 4(b)] while the reverse is true in the downstroke regime [Fig. 4(e)]. This confirms that the intensity differences we observe are not due to problems of alignment in the pressure cell.

Another possible cause for a decrease in PL intensity is due to dislocations that occur near a structural phase transition, seen in several direct gap materials such as CdS (Ref. 5) and CdTe.[21,22] In $Al_{0.3}Ga_{0.7}As$, however, the phase transition takes place[23] at ~ 150 kbar, and is unlikely to cause dislocations at 70 kbar. A characteristic of dislocations is that releasing the pressure does not allow the PL intensity to recover. Since near total recovery is observed at ~ 10 kbar, we conclude that dislocations do not cause the effect seen.

A simple model that describes the effect is a trapping center with lattice relaxation. Since the hysteresis effect is large, it is likely that the lattice relaxation is large as well. A schematic model is shown in a configuration coordinate diagram scheme in Fig. 7. The minimum in the potential energy for the center U_T is displaced from

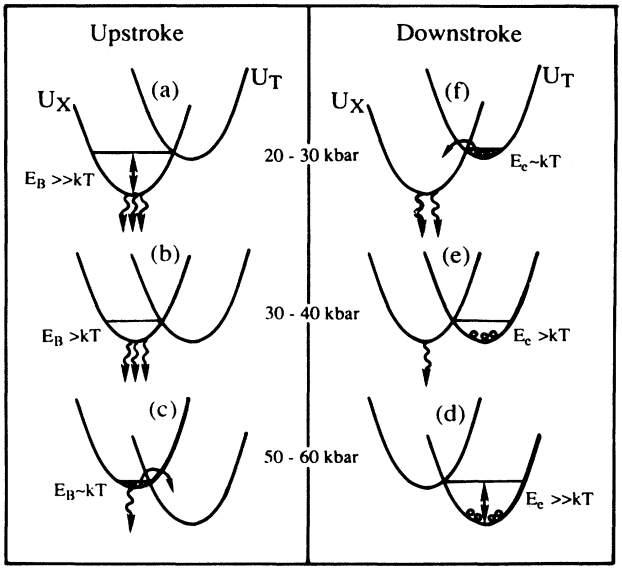

FIG. 7. Configuration coordinate diagram for a large lattice relaxation model. Upstroke regime, left panel: (a) at low pressures $\Delta E \gg kT$ and no electrons scatter to U_T; (b) intermediate pressures, although the bottoms of U_X and U_T line up, $\Delta E > kT$, and still no electrons transfer to U_T; (c) at high pressures $\Delta E \sim kT$ and electrons transfer to U_T and are trapped. Downstroke regime, right panel: (d) at high pressures the emission barrier $E_e \gg kT$ and trapped electrons cannot return to U_X; (e) at intermediate pressures $E_e > kT$ and most electrons remain in U_T; (f) at low pressures $E_e \sim kT$ and electrons repopulate U_X.

that of the hydrogenic-donor state associated with the X CB U_X. It is assumed that the X CB is the feeder level for the deep levels B, C, and D. Scattering to U_T may occur thermally via the capture barrier E_B or via an intermediate state E_m as has been postulated for the DX center.[24] Our data does not make it possible to differentiate between the two processes. For simplicity, we assume that the level that mediates the transfer of electrons from U_X to U_T is separated from the bottom of U_X by an energy ΔE, and the ΔE varies linearly with pressure. We remark that if the transfer of electrons occurred thermally via E_B, ΔE, defined by the intersection of U_T and U_X, would be proportional to P^2. Without knowledge of the exact mechanism, however, a simple linear approximation is justified.

At low pressures between 20 to 30 kbar, U_T is high above the X CB, as is E_m. In this pressure region $\Delta E \gg kT$ for $T=15$ K and no electrons scatter to the center. Strong recombination is observed from electrons that are photoexcited into the X CB [Fig. 7(a)]. At slightly higher pressures ≈ 40 kbar where the bottoms of the potentials line up, there is still no transfer of electrons to U_T since ΔE is still larger than kT [Fig. 7(b)]. At yet higher pressures ~ 50 kbar, U_T is well below U_X, $\Delta E \sim kT$, electrons transfer to the trap, and the PL intensity decreases sharply [Fig. 7(c)]. At the highest pressures ~ 65 kbar, all electrons are transferred to the trap and the PL intensities from all states die below experimentally detectable levels.

On the downstroke, when the pressure is reduced back near 50 kbar where the intensity was initially observed to decline, few electrons recombine radiatively and PL intensity is low [Fig. 7(d)]. The thermal emission barrier for the electrons to escape from the center $E_e \gg kT$ and the trapped electrons cannot return to U_X. Upon decreasing the pressure further to ~ 40 kbar, E_e decreases but is still larger than kT, and most of the electrons remain in U_T [Fig. 7(e)], even though some of the PL intensity is observed to recover. At low pressures [Fig. 7(f)], $E_e \sim kT$ (26 meV) and the center U_T empties out as witnessed by the recovery of PL intensity to prepressurizing levels. We note that even in this simple model, the quenching process and the hysteresis, though arising from the same trapping center, are determined by different quantities. The quenching of PL and the pressure at which it occurs is determined by the crossover energy, the carrier density, and E_B of trapping centers. The hysteresis is determined by the activation energy and kinetics of the center. This difference may allow selective tuning of the quenching and recovery pressures in future experiments.

The upstroke PL intensity $I(P)$ as a function of pressure P was fit to the following equation,[18,19] which has been used to describe the carrier transfer when the Γ and X CB's cross under pressure:

$$I(P)=\frac{I_0}{1+Ae^{\Delta E/kT}}+I_{\min}\ , \tag{1}$$

where $\Delta E=(\alpha_X-\alpha_m)(P-P_T)$ is the energy separation between the mediating level and the X CB, α_m and α_X are their respective pressure coefficients, P_T is the crossover pressure, defined by the pressure at which the energy difference between E_m and the bottom of $U_X \approx kT$, k is Boltzmann's constant, and A is a fitting parameter. From the fit we obtain $P_T=45\pm1$ kbar and $\Delta\alpha=(\alpha_X-\alpha_m)=0.8\pm0.1$ meV/kbar, giving $\alpha_m=-2.4\pm0.3$ meV/kbar, since $\alpha_X=-1.6\pm0.2$ meV/kbar. Similar fits to the MQW sample[12] yield $P_T=47\pm1$ kbar, and $\alpha_m=-3.5\pm0.3$ meV/kbar, values from two different samples that are within two standard deviations of each other. These fits are shown as the solid line in Fig. 5. When Eq. (1) is used for the Γ-X crossover,[18,19] $I_{\min}/I_0=\tau_{\text{scatt}}/\tau_{\text{rad}}$, where τ_{scatt} is the scattering time from the higher to the lower valley, and τ_{rad} is the radiative lifetime. If we assume the same interpretation, this ratio for our system is $\sim 10^{-2}$. Table II lists the parameters obtained from these fits for both the bulk $Al_{0.3}Ga_{0.7}As$ and the MQW sample studied.

This qualitative model for the emptying of electrons from U_T to U_X would predict a sharp recovery curve (dashed lines in Fig. 5) if the temperature was held at 15 K while pressure was reduced. However, some trap emptying occurs because the sample is cycled to 300 K in order to change the pressure. Above 46 kbar, a few electrons transfer out of U_T into U_X and then to the VB. These electrons are photoexcited into U_X at 15 K where most of them transfer back to U_T, while a few undergo radiative recombination. This causes the downstroke curve seen in Fig. 5 to be smoother than the upstroke. Below 46 kbar the photoexcited electrons do not transfer back to U_T since they have too high a capture barrier to overcome in order to scatter into U_T. However, since some electrons are still in U_T, the PL intensity has not yet recovered.

The fact that only a *few* photoexcited carriers participate in radiative recombination in the downstroke regime below 46 kbar is borne out by the change in the line shape of the spectrum. While the 44-kbar spectra for the upstroke and downstroke look alike, with clearly defined A, B, and C peaks [Figs. 4(b) and 4(e)], the upstroke and downstroke spectra at 31 kbar do not [Figs. 4(a) and 4(d)]. Recall that peak A is seen only for high exciting intensities, while B and D are more pronounced for low excitation intensities (Fig. 1). The spectra shown in Fig. 4 were all obtained at the same laser power density of 764 W cm^{-2}. The spectrum seen in Fig. 4(d) looks remarkably like the spectrum seen for a lower power density of 37 W cm^{-2} in Fig. 1. This leads us to conclude that at the higher pressures in the downstroke (44 kbar), there are few states available and the few electrons available populate B, D, and A as well. At lower pressures in the downstroke regime (31 kbar) there are few electrons available, while the number of available states is larger than at 44 kbar. Therefore the electrons preferentially populate the lower-energy levels B, C, and D, and do not populate level A.

The downstroke PL intensity data is fit to Eq. (1) using $\Delta E=\Delta\alpha'(P-P_R)$ at $T=300$ K. A downstroke recovery pressure $P_R=27\pm3$ kbar is obtained, consistent with that observed from the MQW sample studied and the qualita-

TABLE II. Parameters obtained by fitting the intensities of radiative transitions to Eq. (1). $\Delta\alpha$ and P_T refer to the upstroke, while $\Delta\alpha'$ and P_R refer to the downstroke data.

Sample and transition	Stroke	A	$\Delta\alpha$ ($\Delta\alpha'$) (meV/kbar)	P_T (P_R) (kbar)
		$Al_xGa_{1-x}As$ (15 K)		
Main X peak	Up	0.90±0.20	0.76±0.12	44.8
	Down	0.46±0.09	5.12±0.31	27.1
		$GaAs/Al_xGa_{1-x}As$ (80 K)		
$E(X)$	Up	0.64±0.22	1.84±0.21	47.8
	Down	1.09±0.64	4.54±1.06	33.1
Level B	Up	0.83±0.31	1.88±0.32	45.9
	Down	1.03±0.94	6.20±1.92	32.3

tive picture presented by the hysteresis in Fig. 7. A sharp recovery curve is predicted by our model if the pressure were changed at 15 K. This curve is shown in Fig. 5 (dashed lines), generated using $P_R = 27$ kbar, $\Delta\alpha'$, and $T = 15$ K. The data obtained from the fit to the downstroke data is not sensitive enough to separate out competing processes above 46 kbar. It is assumed that the dominant process of trap emptying due to cycling to room temperature prevails over the retransfer of electrons from U_X to U_T. Because of the competing processes, $\Delta\alpha'$ does not directly give the pressure coefficient of the level that mediates the recovery process. However, since $\Delta\alpha'$ is quite different from $\Delta\alpha$, it is possible that the emptying of the center occurs via the thermal E_e while trapping occurs via an intermediate state.

While the microscopic origin of the center is not known at present, we can eliminate certain known centers as being the cause of the phenomenon we observe. The DX center is the first such center that comes to mind. The DX is known to be present in $Al_xGa_{1-x}As$ between $x = 0.22$ and at least[25] 0.74. However, the DX empties at 300 K, and has an $E_e \sim 300$ meV. The fact that this center does *not* empty at 300 K indicates that it is not the normal DX center. Besides, the DX is present already at low pressures, but does not affect the spectra. The work of Brunthaler and Ploog[26] has shown that the DX does not appear to affect PL on the long time scales in time integrated spectra such as ours. Once the DX saturates upon irradiation with light, which can take a few seconds, radiative recombination proceeds as if it were absent. One therefore does not expect the DX to have any further effect on the radiative recombination. All these arguments serve to show that the normal DX is not the cause of the effect we observe.

That the effect occurs at high pressures suggests that the center has an energy that is resonant above the X CB at low pressures and comes below it at high pressures. This is similar to several defect-induced levels, such as the DX in GaAs or the N levels in GaAs, which are metastable and therefore resonant at ambient pressure and then become stable at higher pressures. This center is even higher than the levels mentioned above, so that it appears below the X CB only at 45 kbar. A recently observed level that crosses to come below the X CB at high pressure is the SD level.[27] However, this level has a fairly low emission barrier of 200 meV, and therefore cannot be this center.

A different way to look at the drop in intensity and hysteresis is not so much in terms of energy-level diagrams but in terms of the availability of the shallow-donor or BE^X levels. If the deep center occurs due to the breaking of bonds and the motion of the donor into an interstitial site, that donor would not contribute a shallow-donor level or a donor bound exciton to the states available to the electron. Thus it is both the energetics and the density of available states that will determine the intensities of the transitions. That the recovery of the available shallow levels is important is indicated by the line shapes of the upstroke and downstroke spectra near the recovery pressure, Figs. 4(a) and 4(d) at 32 kbar, and by the energies of the transitions seen in the doped quantum-well sample[12,17] where a similar drop in the PL intensity of the staggered transitions in GaAs-$Al_{0.3}Ga_{0.7}As$ MQW's has been observed.

The DX is indeed postulated to be due to bond breaking and lattice relaxation as described above.[1] In the model, one bond is broken, and the donor captures two electrons and becomes negatively charged. In our case, it is possible that the donor occupies a different interstitial site, which allows it to have a deeper emission barrier than DX. It is also possible that this other interstitial site becomes more favorable because of the additional lattice strain energy provided by the decreased lattice constant under hydrostatic pressure. At the present time no calculations exist for this center.

Our discussions above have assumed that this center is an electron trap. It is well known that at low temperatures PL is dominated by hole trapping.[26] In order to observe this effect, the authors cooled the sample in the dark so that all the electrons were trapped by the DX center (which was lower than the shallow-donor center in their sample). Upon irradiation with light, electrons and holes were available in the CB and VB, respectively. The holes were trapped by the DX center, converting it to the shallow-donor level. This process occurred until all the DX centers were converted to the neutral donor level, a process that took about 20 s (in a sample with 1.5×10^{18} Si/cm^3, 2-μm thick), or roughly as long as it took to irradiate it with as many photons at Si atoms. During this period, the competition between holes being trapped at DX and the holes recombining with electrons causes a gradual rise in the PL intensity to its maximum value $I(\infty)$. Once all the DX's are converted at low temperature, the transient can be repeated only by warming the

sample and repopulating the *DX*.

In our experiment, the time scales of the experiment are considerably longer. No particular care was taken to cool the sample in the dark. Spectra were typically recorded an hour or two after the first irradiation with light. If hole trapping were indeed responsible for the decreased PL intensity when this center becomes active, then it implies that at the time of the measurement we are still on the rising edge of the transient. We conclude this because there appears to be no evidence that the presence of the *DX* center decreases the saturation intensity $I(\infty)$: no such effect has been observed in GaAs PL as one crosses the *DX* center. If the lowered intensity we observe is due to our still being on the rising edge of the transient, it implies hole trapping with a very long time constant, of the order of several hours.

If the center is hole dominated, then the turn-on pressure would have to be the same in GaAs as in $Al_{0.3}Ga_{0.7}As$, in order to account for the identical P_T values that we have observed in the bulk and MQW samples. An electron trap, on the other hand, would not have this requirement, since the conduction state involved in both samples is the $Al_xGa_{1-x}As$ *X* CB. At present P_T in GaAs is not known.

In our studies of the doped MQW, we have observed a sudden shift in the energy of the main staggered peak to a value about 12 meV *higher* at ~40 kbar. We interpret this as a shift from a screened transition below 40 kbar (due to the large number of electrons from the well) to a free exciton above 40 kbar, when all the electrons are trapped. This higher-energy free excitonic transition is preserved in the downstroke. This phenomenon is easier to understand on the basis of electron rather than hole trapping. At present therefore, we feel that there is more evidence to support the idea that the center traps electrons rather than holes. However, more detailed studies are required before the issue is resolved.

As estimate of the position of E_m at ambient pressures can be made from a linear extrapolation. Using average values from Table II of $\Delta\alpha=(\alpha_X-\alpha_m)=-1.3$ meV/kbar, and $P_T=46$ kbar , E_m is 60±26 meV above the *X* CB at ambient pressures. The linear extrapolation has a large uncertainty because the data that describes the pressure coefficient occurs over small range of pressures between 45 and 60 kbar, i.e., in the steep part of the upstroke curve in Fig. 5. From this extrapolation we conjecture that the center may be important at large values of x between $0.7<x<1.0$.

We conclude that the center we have observed is indeed of a different type, and that it has never previously been observed. Its presence in two different samples confirms the belief that it may be generic to $Al_{0.3}Ga_{0.7}As$. It is possible that the center is present at all Al compositions, and that it is active at ambient pressures at large x values. This depends on the role played by the strain energy in determining the stability of the center. We are currently investigating several samples of different Al compositions and dopants to establish the pressures at which the center becomes active at different x's. From these studies we expect to predict whether the center is active at ambient pressures.

Apart from the microscopic origin of the trapping center, there are several other unknowns that are of importance. The most important is the density of traps and whether it is closely related to the number of donors. If it is equal to the number of donors or a multiple, it would indicate a singly or multiply charged donor, respectively. Traditionally, this has been a difficult quantity to measure. The emission and capture barriers and their pressure dependence are also unknown at present. We are currently conducting annealing experiments to determine E_e. Another important quantity is the capture rate of electrons into empty traps and holes into filled traps. These rates will determine the kinetics of steady-state recombination, and are not known at present. Yet another question is whether the traps can be saturated by a higher level of photoexcitation, and therefore alter the pressure at which the PL quenching occurs.

C. Comparison between bulk and quantum-well PL intensities

An interesting question that arises in $GaAs/Al_xGa_{1-x}As$ quantum-well structures, where the indirect transition takes place from the *X* CB of $Al_xGa_{1-x}As$ to the Γ VB of GaAs, is the efficiency with which electrons transfer across the interface.[9] We can estimate the transfer efficiency by comparing the PL intensity in the indirect regime of a bulk $Al_xGa_{1-x}As$ sample to that of a quantum-well sample. Figure 8 shows the PL intensities in the upstroke for peaks *A* and *B* in two samples: the bulk $Al_{0.3}Ga_{0.7}As$ sample (open symbols) and a quantum-well sample (MQW) which consisted of 80

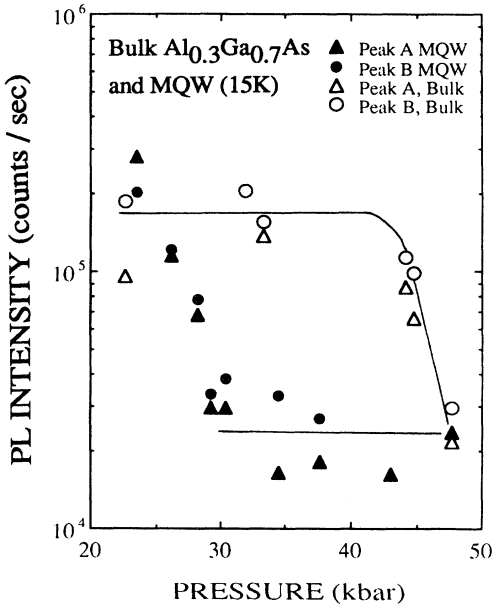

FIG. 8. A comparison of upstroke PL intensities in the indirect regime for the bulk $Al_xGa_{1-x}As$ sample and a MQW sample. The exciting intensities were 15 mW for the bulk and 3.75 mW for the MQW. Owing to saturation at higher powers (Fig. 2), the PL intensity in the MQW is smaller than that of the bulk by a factor of 3 (see text). The difference is indicative of the efficiency with which electrons transfer across the heterointerface. The lines are a guide to the eye.

periods of (40 Å)/(80 Å) GaAs/$Al_{0.3}Ga_{0.7}As$ with center doped wells (10^{18} Si/cm^3), denoted by the solid symbols. The region of interest in Fig. 8 is between 30 and 45 kbar, before the intensity drops due to the trapping center that we observe. In the MQW sample, the region between 20 and 30 kbar shows a decline in intensity, presumably because that is the region where the X CB in GaAs crosses the Γ in GaAs, after which the electron cascade takes the path GaAs Γ CB$\rightarrow$GaAs X CB$\rightarrow$$Al_xGa_{1-x}As$ X CB.

The data shown in Fig. 8 are the raw data taken at 15 K, with 15 mW of excitation power for the bulk sample and 3.75 mW for the MQW. From Fig. 2 we see that the PL intensity is already in the saturation regime at these powers. The fourfold difference in power corresponds to only a twofold increase in the PL intensity for the bulk sample. Corrected for the incident intensity, the radiative efficiency of the MQW is about three times less than that of the bulk sample.

The efficiency of transfer of electrons across the interface should depend on the well width, which affects the penetration of the wave function into the barrier. The relative sample quality is also important when PL intensities are being compared. In the present comparison, the two samples were grown at different times and under slightly different conditions, and therefore the sample qualities cannot be compared. The doping in the MQW sample was able to provide a large number of electrons in the CB. Due to the differences in the samples, the factor of 3 difference in the recombination efficiency should be regarded as an order of magnitude estimate.

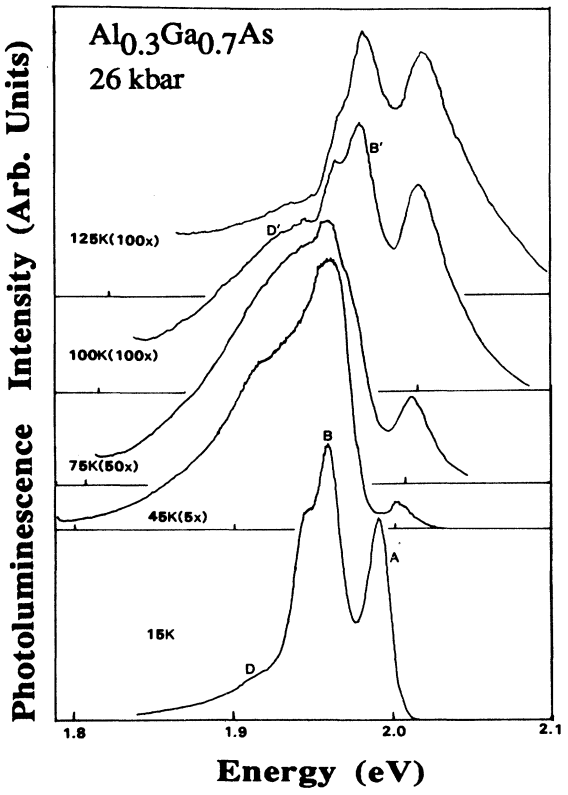

FIG. 9. PL spectra at 26 kbar for several temperatures. The lowest-energy axis corresponds to energies at 15 K. The axes for other temperatures are shifted by an energy equal to the temperature shift of the X band gap.

D. Temperature dependence of radiative transitions

The peak position energies and intensities of the PL spectra obtained from bulk $Al_{0.3}Ga_{0.7}As$ are strongly temperature dependent. To study this dependence, temperature studies were conducted at representative pressures of 1 bar, 6, 26, 33, and 44 kbar. The laser excitation power density was held constant at 764 W cm^{-2} using the 5145-Å line while varying the temperature between 15 and 125 K. An example is seen in Fig. 9, where spectra at a few temperatures are shown at 26 kbar. The energy axes for spectra at temperatures above 15 K have been shifted relative to the 15 K spectrum to compensate for the shift in the band gap with temperature according to the Varshni[28] equation:

$$E(T)=E(0)-\frac{\alpha' T^2}{T+\beta'} , \tag{2}$$

where α' and β' are the Varshni coefficients[29] for the appropriate symmetry points. Values for GaAs are used: $\alpha'=4.6\times10^{-4}$ eV/K and $\beta'=204$ K for X, and $\alpha'=5.405\times10^{-4}$ eV/K and $\beta'=204$ K for the Γ CB.

In the 15 K spectrum peaks A, B, C, and D are easily seen. As the temperature is raised BE^X (A) shifts to higher energies, indicated by A', and lower relative PL intensities. The shift is approximately 12 meV between 15 and 45 K (after compensating for the temperature shift of the band gap), and coincides with the position of FE^X (A') at lower laser powers in Fig. 1. The energy shift indicates an ionization of BE^X to FE^X with temperature, and is consistent with the activation energies to be discussed later. The DA^X levels B and D are almost stationary in energy up to $\sim$75 K, beyond which they decrease in intensity and new peaks, B' and D', 20-meV higher in energy appear. This is consistent with the ionization of the acceptor at the higher temperatures, and conversion of the DA^X transition from a bound-to-bound to a bound-to-free transition. The process is once more corroborated by the activation energies. At 125 K, B' is the dominant level while peak D has disappeared entirely and a weaker peak D' remains.

In order to obtain the activation energies, Lorentz oscillators were fit to the spectra and the integrated intensity for each peak was calculated at each temperature and pressure. A sample fit is shown in Fig. 10. The integrated intensities were plotted as a function of inverse temperature to obtain Arrhenius plots, using the following equation:

$$I(T)=\frac{I_0}{1+\sum_j C_j \exp(-E_{aj}/kT)} . \tag{3}$$

$I(T)$ is the integrated intensity, I_0 is the integrated intensity at $T=15$ K (taken to be the asymptotic value at 0 K), E_{aj} is the activation energy, and $j=1$ or 2 depending

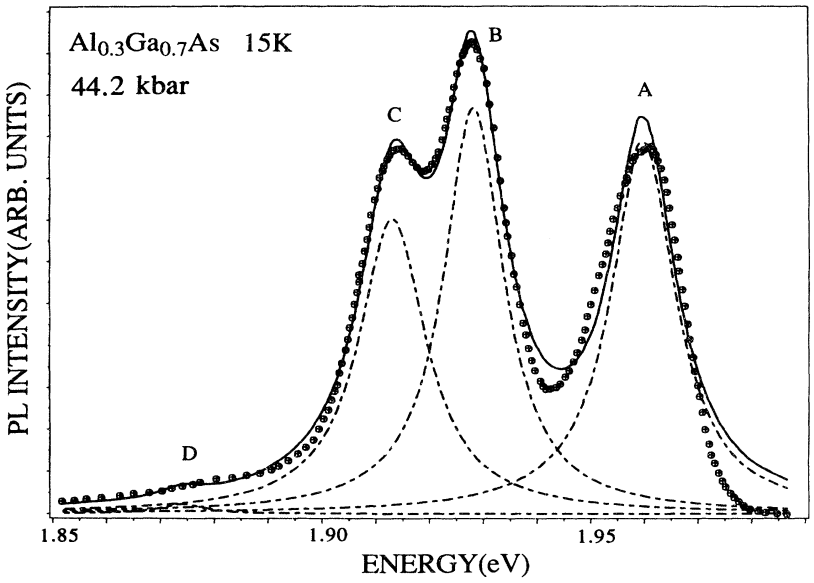

FIG. 10. A Lorentz oscillator fit to the PL spectrum at 44.2 kbar and 15 K for bulk $Al_xGa_{1-x}As$ in the indirect regime. The circles represent the data. The dashed lines are the individual Lorentzians fit to the four peaks, and the solid line is the sum of the four Lorentzians.

on whether one or two activation energies described the energy level. E_{aj} and C_j are used as fitting parameters. Sample Arrhenius plots of the levels associated with the Γ and the X CB's are shown in Figs. 11(a) and 12(a), at 1 and 26 kbar, respectively. For example, in Fig. 12(a) at 26 kbar, the A, $B+C$, and D levels all exhibit similar two-step activation processes in the temperature range 15–125 K. In the Arrhenius plots we used the combined intensities of the B and C peaks, since Fig. 9 shows that as the temperature is raised levels B and C become indistinguishable. This analysis is reasonable if C is considered to be a phonon replica of B, as discussed in Sec. III A. The activation energies E_a obtained for all pressures are listed in Table III.

Figures 11(b) and 12(b) show a plot of the actual peak energy positions (solid lines with data points) and the

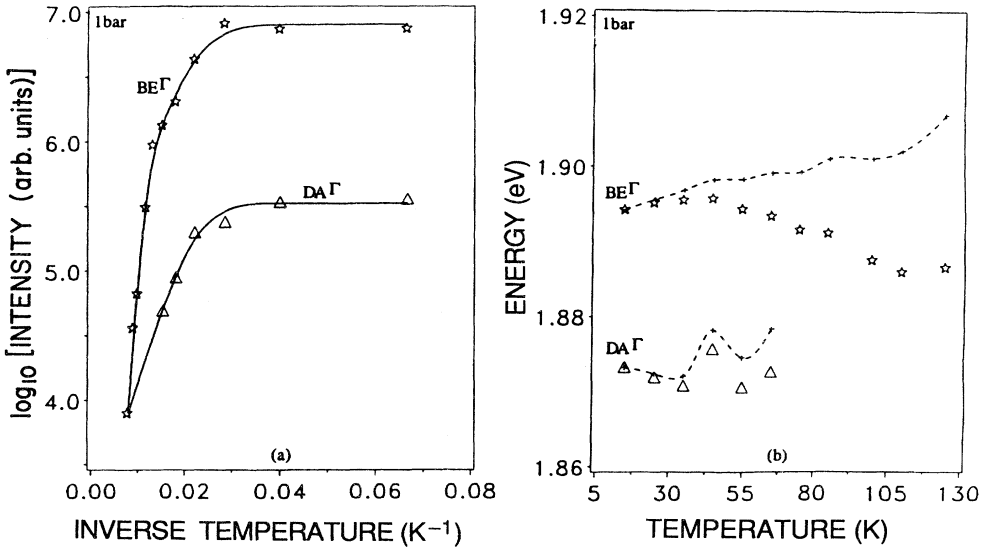

FIG. 11. (a) Arrhenius plots for the Γ bound levels in bulk $Al_{0.3}Ga_{0.7}As$ at 1 bar. The integrated intensities are represented by the data points (BE^{Γ} is the open star and DA^{Γ} is the triangle) and the solid line is a fit to Eq. (3). The activation energies obtained are listed in Table III. (b) Energies of Γ peaks as a function of temperature (BE^{Γ} is the open star and DA^{Γ} is the triangle); the energies corrected for the shift in the band gap with temperature are shown by the dashed lines.

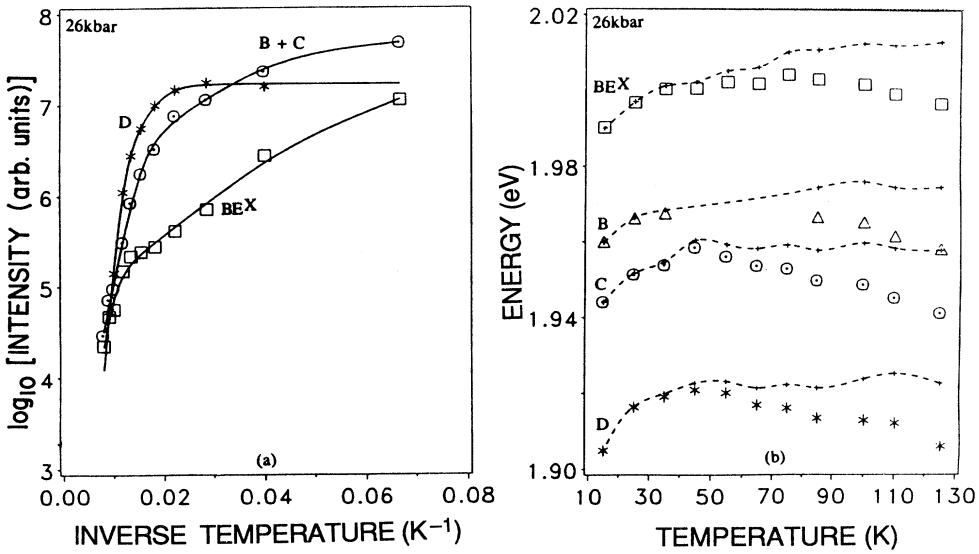

FIG. 12. (a) Arrhenius plots for the X levels in bulk $Al_{0.3}Ga_{0.7}As$ at 26 kbar: BE^X (peak A) is the square, DA^X (peaks $B+C$) is the circle, and DA^X (peak D) is the star. The solid lines are fits to Eq. (3). (b) Energies of X bound peaks as a function of temperature: BE^X is the square, DA^X (B) is the triangle, DA^X (C) is the circle, and DA^X (D) is the star; the energies corrected for the shift in the band gap due to temperature are shown by the dashed lines.

temperature shifted energy positions (dashed lines), which indicate the position of the energy level relative to the 0 K position of the energy bands.

Coupling the information from the activation energies and the energy shifts of the peaks with temperature leads to an understanding of the associated scattering mechanisms listed in Table III, and an associated energy-level diagram,[12] Fig. 13. The scattering processes are shown in Fig. 13 at the appropriate pressure as vertical arrows that start at the initial energy level and terminate an E_a above. When there are two successive activation processes, the arrows corresponding to $E_{a,1}$ and $E_{a,2}$ are stacked vertically. The scattering processes for different energy levels at a single pressure are shown side by side. For the sake of clarity, the uncertainties in the E_a's are not shown. In the indirect region, the energies of the donor levels that give rise to the transitions DA^X (B and D) are shown rather than the transition energies, since it is from these donor levels that the scattering processes occur. These levels are indicated at B_{CB} and D_{CB}, respectively,

TABLE III. Activation energies in $Al_{0.3}Ga_{0.7}As$ at selected pressures.

Pressure	Transition	E_a (meV)	Scattering process
1 bar	BE^Γ	21±5	To Γ CB
		101±11	FE^Γ to L CB
	DA^Γ	23±4	Ionization of acceptor
6 kbar	BE^Γ	21±8	To Γ CB
		85±20	FE^Γ to L CB
	DA^Γ	24±10	Ionization of acceptor
		111±5	Donor to L CB
26 kbar	BE^X (A)	9±1	BE^X to FE^X
		73±17	FE^X to L CB
	DA^X ($B+C$)	9±2	To BE^X (A)
		56±3	DA^X to X CB
	DA^X (D)	30±5	Ionization of acceptor
		116±9	DA^X (D) to X or E_m
33 kbar	BE^X (A)	11±1	BE^X to FE^X
	DA^X ($B+C$)	9±3	To BE^X (A)
		43±5	DA^X to X CB
44 kbar	BE^X (A)	13±4	BE^X to FE^X
		44±13	FE^X to X CB
	DA^X ($B+C$)	19±3	To FE^X (A)
		143±32	To L CB
	DA^X (D)	29±3	Ionization of acceptor

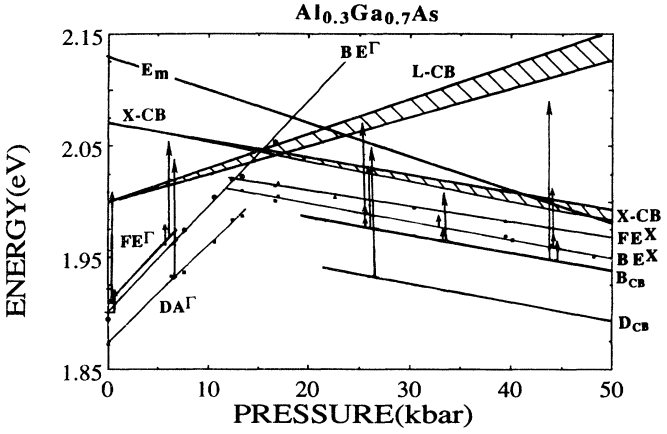

FIG. 13 An energy-level diagram showing the scattering processes listed in Table III. Most of the data points (shown in Fig. 3) have been removed for clarity. In the indirect region, the energies of the donor levels relative to the X CB (rather than the transition energies) that give rise to B and D are shown, labeled B_{CB} and D_{CB}, respectively (see text). The scattering processes are indicated by the vertical arrows at the five pressures listed in Table III. Also shown in this figure is the position of the energy level E_m, which mediates the scattering of electrons from the X associated levels to the trapping center.

Since the transitions B and D terminate on the acceptor, the energy of the donor level relative to the VB is 22 meV (the acceptor binding energy) higher than the respective transition energy. Also shown in Fig. 13 is the position of the state that mediates the trapping, E_m, from a linear extrapolation as described in Sec. III B.

The scattering processes in the direct region are as expected. At 1 bar, the BE^{Γ} scatters to the Γ CB with an $E_{a,1}$ of 21 ± 5 meV at low temperatures, ionizes to the FE^{Γ} around 35 K, then scatters to the L CB with an $E_{a,2}$ of 101 ± 11 meV, consistent with the 15 K Γ-L separation of 110 to 117 meV.[30] The acceptor in DA^{Γ} undergoes ionization with an E_a of 23 ± 4 meV. At 6 kbar the process for BE^{Γ} is the same as that at 1 bar. The DA^{Γ}, however, undergoes a two-step activation process from a bound acceptor to a free valence state with $E_{a,1}$ of 24 ± 10 meV, then scatters to the L CB with an $E_{a,2}$ of 111 ± 5 meV. Presumably the second step of DA^{Γ} scattering is not seen at 1 bar because the L CB is higher in energy. Using the pressure coefficients $\alpha_L=5.5$ meV/kbar[31] and $\alpha_{\Gamma}=9.9$ meV/kbar,[8,9] the Γ-L separation decreases at 6 kbar by 26 meV (to 91 meV), making the L CB more accessible to scattering processes in the temperature range of our measurements.

In the indirect regime, we discuss the 26-kbar data as an example. At 26 kbar, BE^X has $E_{a,1}=9\pm1$ meV, corresponding to scattering to FE^X in the low-temperature region, which is consistent with the 10-meV increase in energy seen in the energy position [Fig. 12(b), dashed lines] and the binding energy of the donor bound exciton. Above 45 K, $E_{a,2}=73\pm17$ meV, consistent with scattering to the L CB. The DA^X levels show a similarly consistent picture. $B+C$ at 26 kbar shows a low-temperature activation energy of $E_{a,1}=9\pm2$ meV, indicating scattering to BE^X (A) between 15 and 40 K. This value of $E_{a,1}$ is in agreement with the separations of the donor levels: the transition energies of A and B at 26 kbar and 15 K are 1.990 and 1.958 eV, respectively. Recalling that B terminates on an acceptor 22 meV above the VB, the donor level of B should be 1.980 eV above the VB, 10 meV below A. Between 40 and 120 K, $E_{a,2}=56\pm3$ meV, which corresponds to scattering of electrons from $DA^X(B+C)$ to the X CB. Again, this value is consistent with the donor-X separation[32] of 45 to 50 meV. Level D has $E_{a,1}=30\pm5$ meV, indicating that the acceptor ionizes at low temperatures, then scatters to the X CB or the mediating level to the trapping center E_m with an $E_{a,2}$ of 116 ± 9 meV. The acceptor binding energy of 22 meV is consistent with C_{As}.

The processes are as expected, scattering to higher donor levels or nearby bands until 44 kbar is reached. At this pressure the scattering processes take a qualitative deviation in their pattern which once again provides evidence for the new deep center discussed in Sec. III B. At 44 kbar, close to the crossing of the trapping center with X, DA^X ($B+C$) shows an $E_{a,1}=19\pm3$ meV where it ionizes to the free exciton FE^X (A') level. In contrast, at 26 and 33 kbar (Table III and Fig. 13) the same level is ionized to the *bound* exciton BE^X (A) with $E_{a,1}\approx10$ meV. This change of scattering channel indicates again that there is a disappearance of available BE^X levels, and is also consistent with the observed switching of radiative energies by 12 meV to FE^X in the MQW sample at ~40 kbar.[12,17] At higher temperatures, DA^X ($B+C$) at 44 kbar scatters to the L CB with an $E_{a,2}=143\pm32$ meV. Again, this is in contrast to the second (higher-temperature) scattering process to the X CB with $E_{a,2}\approx50$ meV at 26 and 33 kbar. DA^X (D) at 44 kbar undergoes a one-step acceptor ionization process with an $E_a=29\pm3$ meV, while at 26 kbar DA^X (D) is observed to have a *two*-step activation process.

Thus, from Arrhenius plots of integrated intensities and Varshni corrections for peak energy positions, scattering processes are proposed and an energy-level diagram is obtained. While these data would not by themselves provide concrete evidence for a trapping center, they are consistent with the existence of the trapping center, and indicate that it originates from above the X CB.

IV. CONCLUSIONS

In summary, we have studied the radiative transitions in bulk $Al_{0.3}Ga_{0.7}As$ at 15 to 125 K under hydrostatic pressures of 0–70 kbar. From these studies we have obtained the following.

(i) The pressure coefficients of all transitions were observed, including free and bound excitons and donor-acceptor-recombination peaks in the indirect regime.

(ii) We have observed a trapping center which causes a pressure-induced hysteresis in the intensity of the indirect radiative transitions. A generic large lattice relaxation model of an electron trapping center is proposed to ex-

plain the data. In this model, the center has an energy about 60±25 meV above the X CB at ambient pressures, and crosses to come below it at 46 kbar. The center has an unusually deep emission barrier and is neither the DX nor the SD center.

(iii) A comparison of the PL intensities of indirect transitions in bulk $Al_xGa_{1-x}As$ and in a quantum-well sample indicates that the PL intensity is about a factor of 3 lower in the quantum well, and provides an estimate of the transfer efficiency of electrons across the heterointerface.

(iv) A study of the temperature dependence of the PL intensities at selected pressures provides activation energies of various levels and a picture of the scattering processes involved, which is consistent with the trapping center becoming active near 45 kbar.

ACKNOWLEDGMENTS

This work was supported by the U. S. Army Research Office under Grant No. DAAL03-86-K0083, the U. S. Department of Energy under Grant No. DE-FG02-84ER45402, and the University of Missouri Research Council. We thank J. Farmer for useful discussions, and J. R. Whitlock for help in fitting the spectra with the Lorentz-oscillator model.

*Present address: AL/OEDL, Brooks Air Force Base, TX 78235-5000.

[1]D. J. Chadi and K. J. Chang, Phys. Rev. B **39**, 10063 (1989), and references therein.

[2]P. M. Mooney, J. Appl. Phys. **67**, R1 (1990).

[3]D. V. Lang and R. A. Logan, Phys. Rev. Lett. **39**, 635 (1977).

[4]N. Chand, T. Henderson, J. Klem, W. T. Masselink, R. Fischer, Y. C. Chang, and H. Morkoç, Phys. Rev. B **30**, 4481 (1984).

[5]U. Venkateswaran and M. Chandrasekhar, Phys. Rev. B **31**, 1219 (1985).

[6]R. Dingle, Inst. Phys. Conf. Ser. **33**, 210 (1977).

[7]V. Swaminathan, J. L. Zilko, W. T. Tsang, and W. R. Wagner, J. Appl. Phys. **53**, 5163 (1982).

[8]M. Chandrasekhar, U. Venkateswaran, H. R. Chandrasekhar, B. A. Vojak, F. A. Chambers, and J. M. Meese, in *Proceedings of the XVIII International Conference on the Physics of Semiconductors, Stockholm, 1986,* edited by O. Engström (World Scientific, Singapore, 1987), p. 943; U. Venkateswaran (unpublished).

[9]U. Venkateswaran, M. Chandrasekhar, H. R. Chandrasekhar, B. A. Vojak, F. A. Chambers, and J. M. Meese, Phys. Rev. B **33**, 8416 (1986).

[10]N. Lifshitz, A. Jayaraman, R. A. Logan, and R. G. Maines, Phys. Rev. B **20**, 2398 (1979).

[11]M. Prakash, M. Chandrasekhar, H. R. Chandrasekhar, I. Miotkowski, and A. K. Ramdas, Phys. Rev. B **42**, 3586 (1990).

[12]W. P. Roach, Ph.D. thesis, University of Missouri, 1990; W. P. Roach, M. Chandrasekhar, H. R. Chandrasekhar, and F. A. Chambers, Phys. Rev. B **43**, 12 126 (1991).

[13]M. Mizuta, M. Tachikawa, H. Kukimoto, and S. Minomura, Jpn. J. Appl. Phys. **23**, L143 (1985).

[14]M. F. Li, P. Y. Yu, E. R. Weber, and W. Hansen, Phys. Rev. B **36**, 4531 (1987).

[15]M. F. Li, P. Y. Yu, E. R. Weber, and W. Hansen, Appl. Phys. Lett. **51**, 349 (1987).

[16]D. K. Maude, J. C. Portal, L. Dmowski, T. Foster, L. Eaves, M. Nathan, M. Heiblum, J. J. Harris and R. B. Beall, Phys. Rev. Lett. **59**, 815 (1987).

[17]W. P. Roach, M. Chandrasekhar, H. R. Chandrasekhar, F. A. Chambers, G. Devane, and K. A. Stair, *Proceedings of the IV International Conference on High Pressure in Semiconductor Physics, 1990,* Porto Carras, edited by D.S. Kyriakos and O. E. Valassiades (Aristotle University, Thessaloniki, 1990), p. 242.

[18]P. Y. Yu and B. Welber, Solid State Commun. **25**, 209 (1978).

[19]D. Olego, M. Cardona, and H. Müller, Phys. Rev. B **22**, 894 (1980).

[20]D. J. Wolford, Inst. Phys. Conf. Ser. **65**, 477 (1983).

[21]D. J. Dunstan, B. Gil, and K. P. Homewood, Phys. Rev. B **38**, 7862 (1988).

[22]M. Prakash, M. Chandrasekhar, H. R. Chandrasekhar, I. Miotkowski, and A. K. Ramdas, in Properties of II-VI Semiconductors, edited by F. J. Bartoli, H. F. Schaake, and J. F. Schetzina, MRS Symposia Proceedings No. 161 (Materials Research Society, Pittsburgh, 1990), p. 449.

[23]B. A. Weinstein, S. K. Hark, R. D. Burnham, and R. M. Martin, Phys. Rev. Lett. **58**, 781 (1987).

[24]T. N. Theis and P. M. Mooney, *Impurities, Defects and Diffusion* in Semiconductors, edited by D. J. Wolford, J. Berholc, and E. E. Haller, MRS Symposia Proceedings No. 163 (Materials Research Society, Pittsburgh, 1990) p. 729.

[25]P. M. Mooney, G. A. Northrup, T. N. Morgan, and H. G. Grimmeiss, Phys. Rev. B **37**, 8298 (1988).

[26]G. Brunthaler and K. Ploog, Phys. Rev. Lett. **63**, 2276 (1989).

[27]Y. B. Jia and M. F. Li, J. Appl. Phys. **66**, 5632 (1989).

[28]Y. P. Varshni, Physica **39**, 149 (1967).

[29]D. E. Aspnes, Phys. Rev. B **14**, 5331 (1976).

[30]H. C. Casey and M. B. Panish, *Heterostructure Lasers* (Academic, New York, 1978), Parts A and B; H. J. Lee, L. Y. Juravel, and J. C. Wooley, Phys. Rev. B **21**, 659 (1980).

[31]A. K. Saxena, Phys. Status Solidi **105**, 777 (1981).

[32]In calculating this separation, we assume that BE^X is 10 meV below FE^X, which in turn has a binding energy of 25 to 30 meV relative to the X CB.